Molecular Simulation
Vol. 34, Nos. 10–15, September–December 2008, 989–995

Taylor & Francis
Taylor & Francis Group

Simulating the structure of amorphous $Si_{0.5}C_{0.5}$ using Lin–Harris molecular dynamics

L.M. Mejía Mendoza[a], R.M. Valladares[b] and Ariel A. Valladares[a]*

[a]*Instituto de Investigaciones en Materiales, Universidad Nacional Autónoma de México, México, Mexico;* [b]*Facultad de Ciencias, Universidad Nacional Autónoma de México, México, Mexico*

(*Received 31 January 2008; final version received 4 September 2008*)

We have amorphised $Si_{0.5}C_{0.5}$ by *ab initio* generating random networks with the experimental density of 2.75 g/cm^3. Two types of crystalline supercells were used at the start: one was a diamond-like periodic supercell of 64 atoms, containing 32 carbons and 32 silicons, chemically ordered, amorphised using Fast Structure®, and the other was an fcc crystalline periodic supercell with 108 atoms, 54 carbons and 54 silicons, chemically ordered, amorphised using DMol^3 from the suite in Materials Studio 3.2®. The amorphisation is made by heating the periodic samples to just below the melting point (the undermelt–quench approach), and then cooling them down to 0 K. Then the structures are relaxed by annealing and quenching, and finally a geometry relaxation is carried out. Our simulations show that Cerius^2® and Materials Studio 3.2 give equivalent results in general: atoms of one kind are almost completely surrounded by the atoms of the other kind. We also find that the two codes lead to total and partial radial distribution functions such that after weighting them with the corresponding experimental structure factors yield curves that are similar and comparable with experiment. Also C—C bonds with an average bond length of 1.35 Å are found.

Keywords: amorphous silicon carbide; *ab initio* molecular dynamics; radial distribution functions

1. Introduction

Recently, we have developed a thermal procedure to generate structures of pure and hydrogenated silicon [1], carbon [2], silicon–nitrogen [3] and carbon–nitrogen [4], and preliminary studies of silicon–germanium, indium–selenium and silicon–carbon have been carried out [5]. All these were generated using Fast Structure (Fast for short) (a code from the Cerius^2® suite), an *ab initio* Harris functional-based program developed by Molecular Simulations, Inc. [6]; our results agree quite well with the experimental data, whenever the comparison is possible. This method has been applied to a low-density (1.8 g/cm^3) sample of $Si_{0.5}C_{0.5}$ successfully [5]; there it was found that silicon atoms tend to form linear chains while carbon atoms tend to form rings and that this low-density sample has a tendency to form homonuclear bonds. Now, in order to investigate the adequacy of the new codes in the Materials Studio 3.2® suite we used DMol^3, with the simulated annealing option, to perform an amorphisation of an fcc supercell of $Si_{0.5}C_{0.5}$ to be compared with a previous calculation of a diamond-like structure of $Si_{0.5}C_{0.5}$ done using Fast. The density used in both simulations is the experimental value reported by Ishimaru and co-workers [7,8], 2.75 g/cm^3.

Several experimental works concerning the characterisation of the structure of a-$Si_{0.5}C_{0.5}$ can be found in the literature [9], and the general conclusion is that only C—Si (heteronuclear) bonds exist in their samples. However, Meneghini et al. [10] have shown that a small percentage of C—C bonds exist although there is a tendency to chemical order for concentrations in the vicinity of a-$Si_{0.5}C_{0.5}$. More recently, Ishimaru and co-workers [7], performing heavy ion bombardment (Ar^+ with energies of 200 keV) on a crystalline wafer of silicon carbide, have produced the amorphous structure of silicon carbide and have studied it using transmission electron microscopy and molecular dynamics simulations. They have shown that the number of heteronuclear bonds increases as the structure of the sample is relaxed; that is, chemical order increases as the annealing progresses. Later on, Ishimaru [8] performed Xe^+ bombardment at 300 keV on a crystalline wafer of silicon carbide originally at 120 K in order to obtain an amorphous layer on the wafer. He characterised this material using transmission electron microscopy and concluded that both homonuclear and heteronuclear bonds exist.

Theoretical studies have been performed in order to understand the atomic topology of this alloy. Kelires [11] has carried out several works using continuous space Monte Carlo and the Tersoff potential [12], and concludes that a-$Si_{0.5}C_{0.5}$ presents some chemical order, C—C homonuclear bonds and threefold coordinated carbon. Similar conclusions were reached by Tersoff [12] who finds that amorphous silicon carbide presents moderate chemical order. Finocchi et al. [13] pointed out that a-$Si_{0.5}C_{0.5}$ has no chemical order at all. However, Tersoff [12] argued that 15% of C atoms in the simulation of Finocchi et al. were

*Corresponding author. Email: valladar@servidor.unam.mx

ISSN 0892-7022 print/ISSN 1029-0435 online

DOI: 10.1080/08927020802454844
http://www.informaworld.com

segregated into graphitic regions; excluding this graphitic regions from the total statistics, he inferred that a moderate chemical order exists in the structure. Ivashenko et al. [14] pointed out that the final structure of a-$Si_{0.5}C_{0.5}$ depends on the initial configuration and that a strong chemical order exists. Rino et al. [15], performing molecular dynamics simulations with an effective two- and three-body interaction potential, concluded that neither carbon nor silicon structures are present under 3 Å; so they state that there is a strong chemical order in these samples. Very recently, Devanathan et al. [16], doing molecular dynamics with a Brenner-type bond order potential [17], have shown that amorphous silicon carbide generated by quenching from the melt has a ratio of 6:13% of C—C homonuclear bonds.

It is clear that there are discrepancies in the literature concerning the presence of chemical order in amorphous silicon carbide, both for simulations and with experiment. It would be desirable to carry out amorphisations that would contribute to clarify the discrepancies and to foster the experimental work on the subject.

2. Method

In our previous simulations, we have used Fast [6], a code found in the Cerius[2] package, based on the Harris functional [18], designed originally for finding in a rapid manner the geometrical structures of atom aggregates by initially disrupting the starting structure and then doing some simulated annealing to allow the aggregate to reach a local energy minimum. In the Materials Studio package, version 3.2, the option of simulated annealing in DMol[3] [19] has the Harris functional option implemented, but does not contemplate the original disruption of the structure so we have to incorporate something equivalent; this we do by starting from a structure that is far from the most stable one. In addition, DMol[3] does not have in the graphical interface the option of simulated annealing by linearly increasing the temperature, so the calculations made in DMol[3] were conducted in *stand alone* mode. Both are DFT codes and they have integrated optimisation techniques based on a fast force generator to allow simulated annealing molecular dynamics studies with quantum force calculations [20]. We use the LDA parameterisation due to Vosko et al. [21] in both cases.

The amorphising of the diamond supercell structure with 64 atoms was performed using Fast and the 108-atom fcc supercell was performed with DMol[3]. In both cases, the core is taken as full, which means that an all-electron calculation is carried out, and for the amorphisation process a standard basis set of atomic orbitals was chosen in Fast and a double numerical basis set of atomic orbitals in DMol[3], with a cut-off radius of 4 Å in both cases. The physical default time step is given by $\sqrt{m_{\min}/5}$, where $m_{\min}$ is the value of the smallest mass in the system, carbon, and this leads to a time step of 1.6 fs. However, in order to increase the dynamical processes that occur in the amorphisation in reasonable computer time, a time step of 4 fs was used. The forces are calculated using rigorous formal derivatives of the expression for the energy in the Harris functional, as discussed by Lin and Harris [19]. We want to compare the way the amorphising processes work for both codes, Fast and DMol[3].

Our process is not designed to reproduce the way an amorphous material is grown, but has the objective of generating an amorphous sample that adequately represents those obtained experimentally. We amorphised the crystalline diamond structure with 32 carbon atoms and 32 silicon atoms in the cell and a density of 2.75 g/cm^3, also the crystalline fcc structure with 54 carbons and 54 silicons–both with periodic boundary conditions, and chemically ordered. It is noteworthy to say that this process is done at constant density. We slowly heated both supercells from 300 to 2800 for the diamond and 3053 K for the fcc, just below their melting points [22], in 100 steps of 4 fs each step, and immediately cooled them down to 0 K in 111 steps for the diamond structure and 112 steps for the fcc. The heating/cooling rate was 6.25×10^{15} K/s for the diamond structure and 6.88×10^{15} K/s for the fcc structure. The atoms were allowed to move within each cell of volume (9.1846 Å)^3 for diamond and (10.9643 Å)^3 for the fcc. We next subjected them to annealing cycles at 300 K for the 64-atom sample and 600 K for the 108-atom sample, with intermediate quenching processes. At the end, a geometry optimisation was carried out to find the local energy minimum of the amorphous structures.

To compare with the experimental results of Ishimaru and co-workers [7,8], the pRDFs obtained in this work were weighted using experimental electron atomic structure factors and then added to obtain the total RDF. For the binary alloy, the precise way to obtain the weighted total RDF is given by the equation [23]:

$$g(r) = \frac{f_x f_x n_x n_x}{\langle f \rangle^2} g_{xx}(r) + 2\frac{f_x f_y n_x n_y}{\langle f \rangle^2} g_{xy}(r) + \frac{f_y f_y n_y n_y}{\langle f \rangle^2} g_{yy}(r), \quad (1)$$

where $(n_x f_x + n_y f_y)^2 = \langle f \rangle^2$, n_x is the atomic fraction of element x, f_x is the atomic structure factor for element x and $g_{xy}(r)$ represents the pRDFs of the x–y elements.

3. Results and discussion

The structures obtained using Fast and DMol[3], after a geometry optimisation, are shown in Figures 1 and 2 for the 64- and 108-atom samples, respectively. Figure 1(a) and (b) are carbon and silicon structures, respectively, inside the 64-atom silicon carbide sample. Figure 1(c)

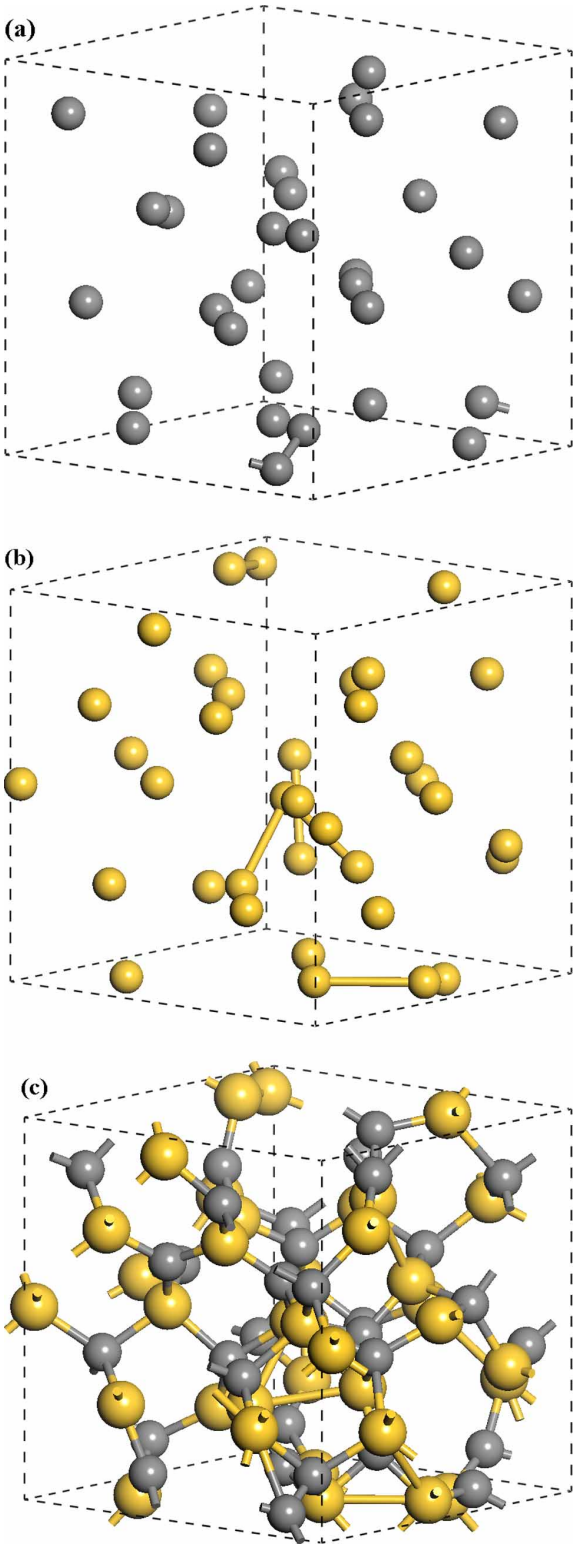

Figure 1. Structures of the amorphous silicon carbide generated by FAST. (a) Thirty-two atoms of a carbon structure inside a-$Si_{0.5}C_{0.5}$, (b) 32 atoms of silicon inside the amorphous structure and (c) 64-atom structure of amorphous silicon carbide with experimental density of 2.75 g/cm^3. There are chain structures of carbon with an interatomic distance of about 1.35 Å.

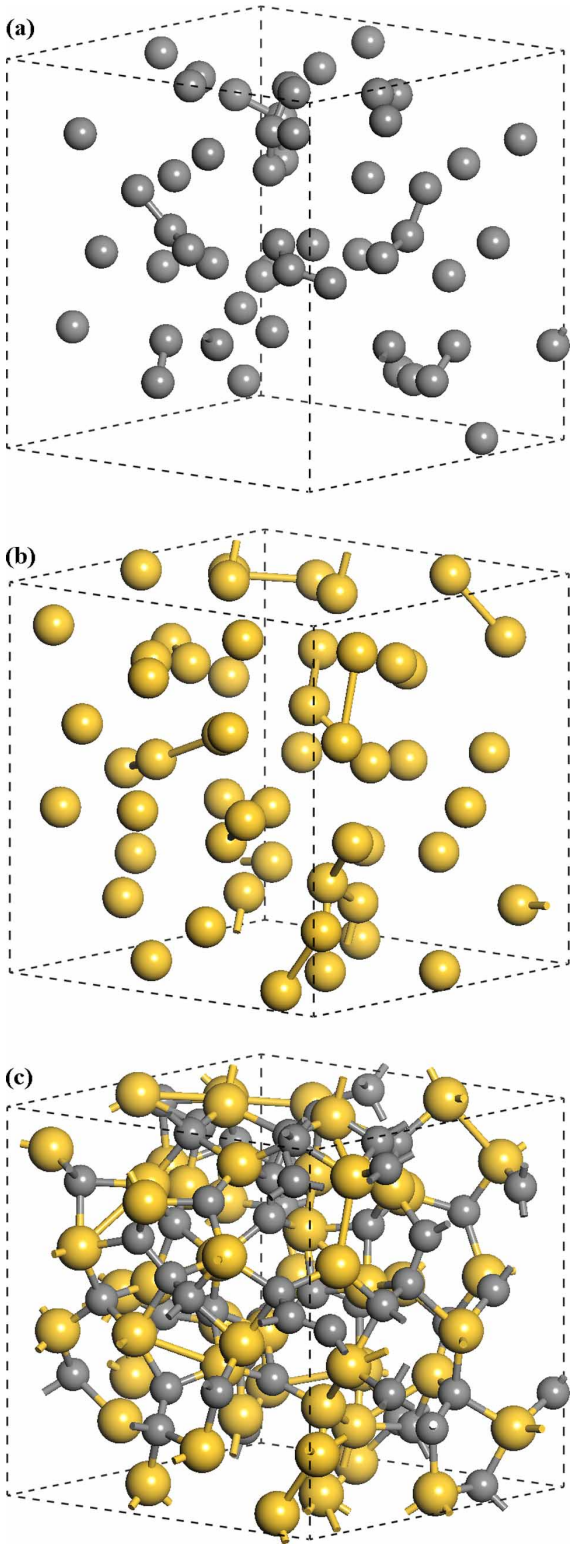

Figure 2. Structures of the 108-atom amorphous silicon carbide generated by DMol^3. (a) Fifty-four atoms of a carbon structure inside a-$Si_{0.5}C_{0.5}$, (b) 54 atoms of silicon inside the amorphous structure and (c) amorphous 108-atom structure of silicon carbide with experimental density of 2.75 g/cm^3. Carbon structures show chain-like configurations, with an average distance of 1.40 Å.

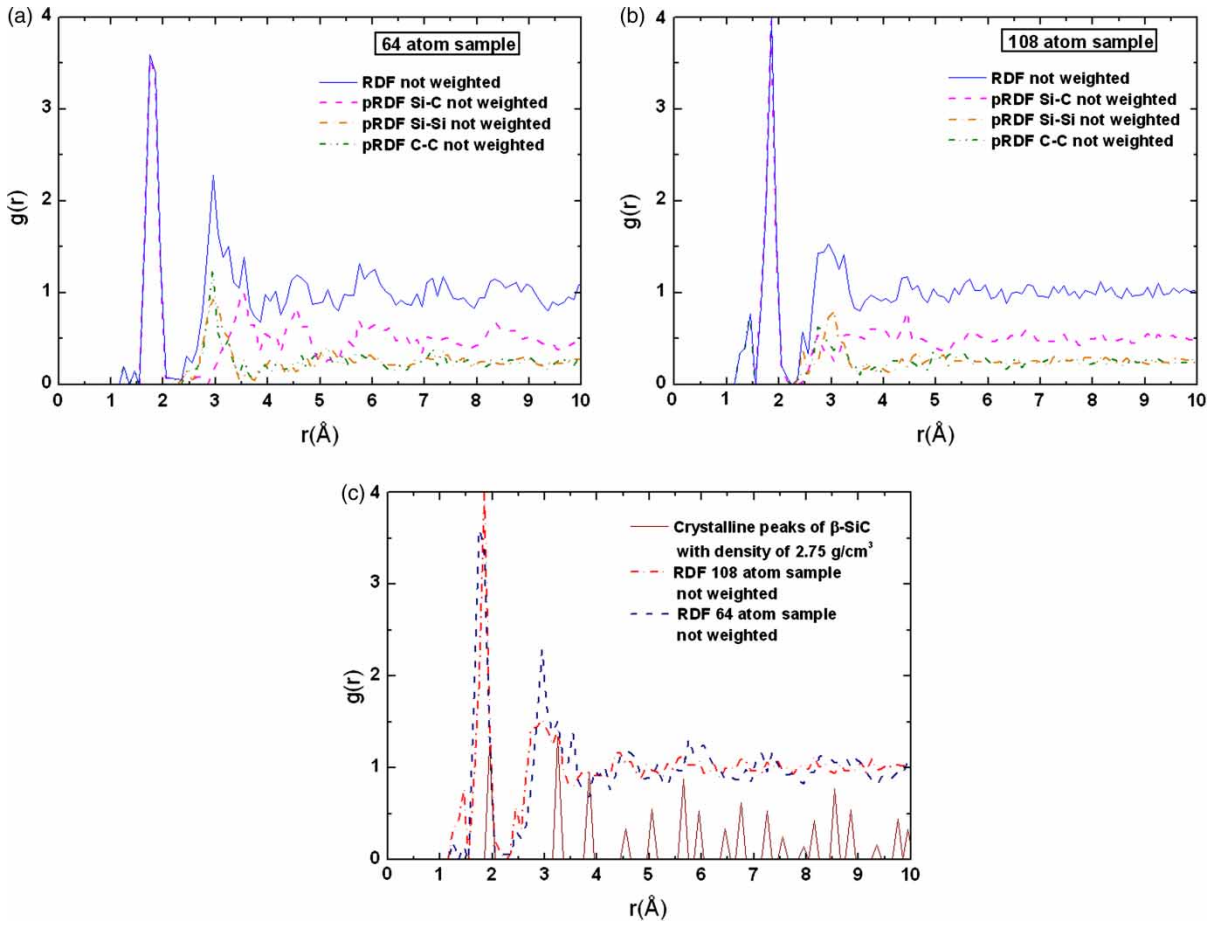

Figure 3. (a) pRDFs and RDF of the 64-atom sample of amorphous silicon carbide generated by our amorphisation process using FAST. (b) pRDFs and RDF of the 108-atom sample with the same amorphisation process using DMol^3. (c) Comparison among the simulated RDFs and the crystalline positions.

is the amorphous structure of silicon carbide generated by our process using Fast. Figure 2(a) and (b) are carbon and silicon structures, respectively, inside the 108-atom sample, whereas Figure 2(c) is the amorphous structure of silicon carbide obtained using DMol^3. In both cases, it can be seen that there are chain-like structures in carbon and silicon, suggesting that there cannot be a complete chemical order. The maximum length of the bonds in Figure 1 was determined as the distance at which the first minimum occurs in the corresponding pRDF in the graphs of Figure 3. For the 64-atom sample, generated with Fast, we have the maximum length of the C—C bonding as the corresponding first minimum of the C—C pRDF in Figure 2(a): 1.55 Å (tetrahedral carbon). The maximum bond length for silicon is given by the position of the first minimum in the pRDF Si—Si: 2.55 Å. Finally, the Si—C maximum bond length, according the first minimum in the pRDF is 2.25 Å. For the 108-atom sample, generated by DMol^3, we have that the minimum in the pRDF C—C is 1.55 Å, pRDF Si—Si is 2.55 Å and pRDF Si—C is 2.55 Å. The maximum lengths of the bonds are the same for both structures. It is clear then that there is some degree of chemical order but far from 100%.

Figure 3 shows the RDFs and the pRDFs for both the 64- and 108-atom samples. In Figure 3(a), total and partial RDFs for the 64-atom sample are shown; the first peak of the C—C pRDF has a bimodal structure: the two peaks are located at 1.25 and 1.45 Å, giving an average position of 1.35 Å; the second neighbour peak for pRDF C—C is at 2.95 Å. Also in Figure 3(a), the first peak of the pRDF Si—C shows a structure with two clear contributions, one at 1.75 Å and the other at 1.85 Å, whereas in the crystalline β-SiC this peak is at 1.88 Å. In Figure 1(a), it is clear that there are some carbon–carbon bonds for the bond length used, so we can say that there exist carbon atoms that, because of the interatomic distances found, could

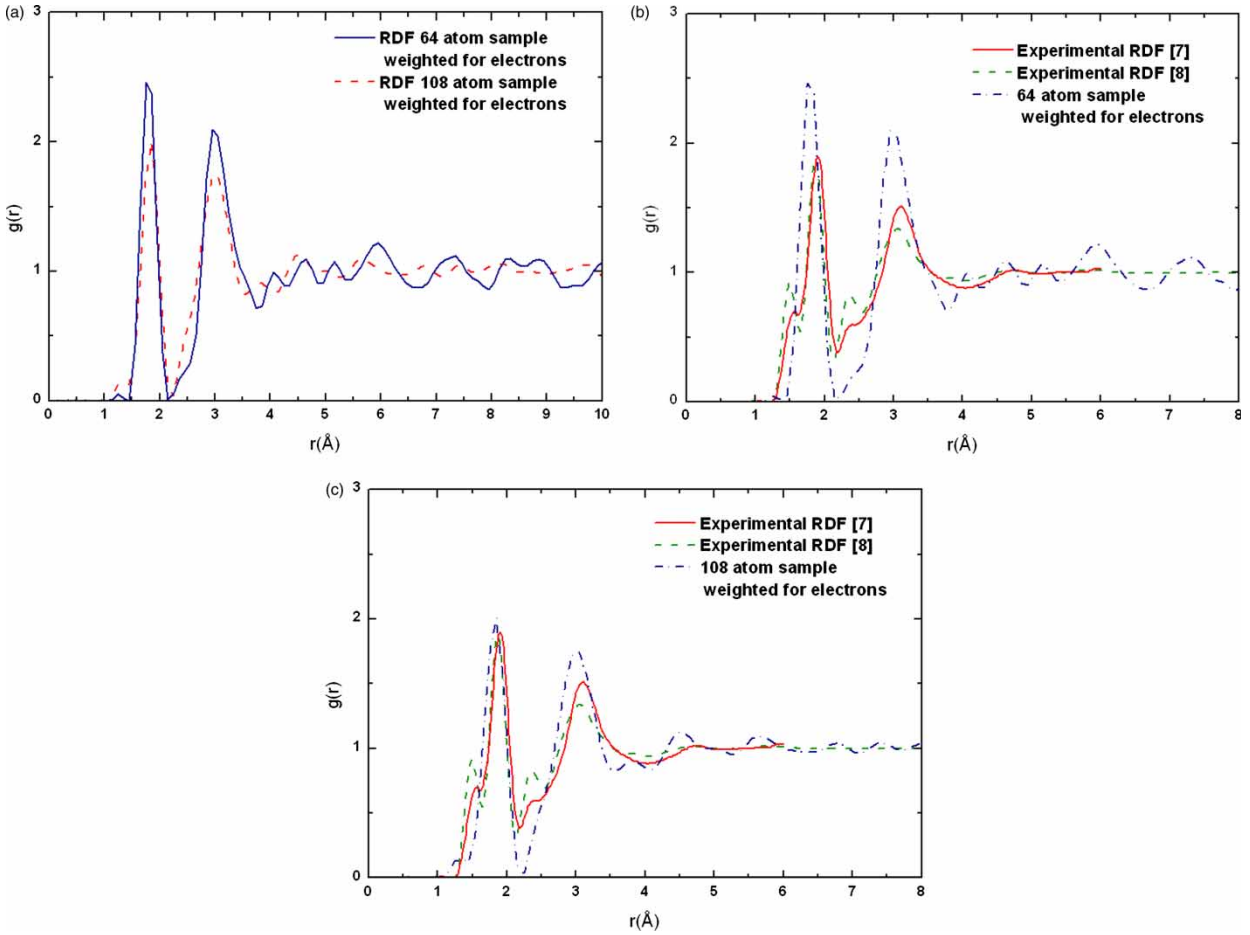

Figure 4. (a) Comparison between the two total RDFs obtained by our processes. (b) Comparison between the experimental RDFs [7,8] and the 64-atom RDF generated by Fast. (c) Comparison between the experimental RDFs [7,8] and the DMol^3-simulated sample of 108 atoms. Here all the RDFs were weighted for electrons and were Fourier smoothed for a better comparison with experiment.

be double-bonded C═C. For the pRDF Si—Si in Figure 3(a), there is a shoulder at 2.45 Å, reminiscent of the local environment in crystalline silicon. The second peak is located at 2.95 Å.

In Figure 3(b), which is our simulation for 108 atoms, the first peak of the pRDF C—C also shows two sub-peaks, one located at 1.25 Å and the other at 1.45 Å. The second neighbour peak for pRDF C—C is at 2.75 Å. For the pRDF Si—C, the first peak is at 1.85 Å; compare with the Si—C structure in the 64-atom sample. Apparently, when there are more atoms in the sample, the major structural contribution in the Si—C peak is at 1.85 Å. The pRDF Si—Si in 108 sample has a first peak at 2.45 Å, and a second peak at 3.05 Å.

Finally, in Figure 3(c) the two total RDFs and the crystalline RDF corresponding to the β-SiC silicon carbide structure are shown; the density of the samples is 2.95 g/cm^3, which is the experimental one [7,8]. From these figures, it can be seen that the 108 atom total RDF is smoother than the 64-atom sample. It can be seen that the average positions of the major peaks essentially coincide, thus the amorphisation process that we have developed works well and gives similar results when used with both computational codes, Fast and DMol^3.

In Figure 4, there is a comparison between the experimental RDFs and the simulated ones weighted for electrons, where the structure factors used can be found elsewhere [24]. In Figure 4(a), the comparison between the total RDF of the 64-atom sample generated with Fast and the total RDF of the 108-atom sample generated with DMol^3 is shown. These graphs were Fourier smoothed to have adequate curves to allow comparison with experiment, since the number of atoms in the cells lead to statistical fluctuations that are not representative of the bulk. Figure 4(b) is the plot of the two experimental [7,8] and the simulated 64-atom total RDFs. The positions of the

peaks reported in [7] are: the C—C peak is at 1.51 Å for the nearest neighbours, whereas the second peak, Si—C, is at 1.90 Å the Si—Si shoulder is at 2.40 Å and the third prominent peak is around 3.2 Å. The same structure prepared under different conditions [8] shows: the C—C peak is at 1.50 Å for the nearest neighbours, whereas the second peak, Si—C, is around 1.88 Å, the Si—Si shoulder is around 2.35 Å and the third prominent peak is around 3.05 Å. As mentioned before, the simulated peaks are a bimodal peak with 1.35 Å and 1.45 Å or 1.35 Å once smoothed; first prominent peak is at 1.8 Å, Si—Si shoulder is at 2.45 Å and the third prominent peak is around 2.95 Å. Figure 4(c) is the plot of the two experimental [7,8] and the simulated 108-atom total RDFs. The peak positions of our 108-atom sample are: bimodal C—C peak is at 1.25 and 1.45 Å, once smoothed this peak is at 1.40 Å; the first prominent peak, Si—C, is at 1.85 Å, a Si—Si shoulder appears at 2.45 Å.

4. Conclusion

We were able to generate, from first principles, random structures that have similar features and that are in qualitative agreement with the experiment. This was done by a recently developed process, the undermelt-quench process, which seems to work for Fast and DMol^3, using the Harris approximation. The results of these simulations reveal the presence of C—C bonds at an average distance of 1.35 Å for the Fast calculation, and the same structure is seen at an average position of 1.40 Å in DMol^3. The results obtained here indicate that a-$Si_{0.5}C_{0.5}$ presents some degree of chemical order and also homonuclear bonds of Si—Si and C—C, in agreement with [7,8]. This suggests that carbon may form chain structures in the simulated samples.

Fast is a code that starts disrupting the atomic structure to begin looking for the local energy minimum. Since the Materials Studio3.2 suite does not have Fast within its codes, one has to find a way around the absence of the original disruption created by this code, and so far we have discovered that one way around this limitation is the use of crystalline supercells that initially are far from equilibrium, so when the process starts, there is an immediate rearrangement of the atoms that inhibit re-crystallisation. Therefore, structures that are not initially in equilibrium may be a way to go to be able to use Materials Studio.

Acknowledgements

LMMM acknowledges the financial support of CONACyT during his PhD studies. RMV and AAV are grateful to DGAPA-UNAM for the funding of their scientific projects. M.T. Vazquez and S. Jimenez provided the information requested.

References

[1] A.A. Valladares, F. Alvarez, Z. Liu, J. Stitch, and J. Harris, Ab initio *studies of the atomic and electronic structure of pure and hydrogenated a-Si*, Eur. Phys. J. B 22 (2001), pp. 443–453.

[2] F. Alvarez, C.C. Díaz, R.M. Valladares, and A.A. Valladares, Ab initio *generation of amorphous carbon structures*, Diam. Rel. Mat. 11 (2002), pp. 1015–1018.

[3] F. Alvarez and A.A. Valladares, *First-principles simulations of atomic networks and optical properties of amorphous SiN_x alloys*, Phys. Rev. B. 68 (2003), 205203. See also F. Alvarez, A.A. Valladares, *Atomic topology and radial distribution functions of a-SiN_x alloys:* ab initio *simulations*, Solid State Comm., 127 (2003), pp. 483–487.

[4] A.A. Valladares and F. Álvarez-Ramírez, *Bonding in amorphous carbon-nitrogen alloys: A first principles study*, Phys. Rev. B 73 (2006), 024206.

[5] E.Y. Peña, M. Mejía, J.A. Reyes, R.M. Valladares, F. Álvarez, and A.A. Valladares, *Amorphous alloys of $C_{0.5}Si_{0.5}$, $Si_{0.5}Ge_{0.5}$ and $In_{0.5}Se_{0.5}$: Atomic topology*, J. Non-Cryst. Solids 338–340 (2004), pp. 258–261.

[6] *FastStructure_SimAnn User Guide, Release 4.0.0*, Molecular Simulations, Inc., San Diego, September (1996)

[7] M. Ishimaru, I.-T. Bae, Y. Hirotsu, S. Matsumura, and K.E. Sickafus, *Structural relaxation of amorphous silicon carbide*, Phys. Rev. Lett. 89 (2002), 055502.

[8] M. Ishimaru, *Electron-beam radial distribution analysis of irradiation-induced amorphous SiC*, Nucl. Instr. Meth. B 250 (2006), pp. 309–314.

[9] P.I. Rovira and F. Alvarez, *Chemical (dis)order in a-Si_{1-x} C_x:H for $x < 0.6$*, Phys. Rev. B 55 (1997), pp. 4426–4434; A. Sproul, D.R. McKenzie, and D.J.H. Cockayne, *Structural study of hydrogenated amorphous silicon–carbon alloys*, Philos. Mag. B, 54 (1986), pp. 113–131; A.E. Kaloyeros, R.B. Rizk, and J.B. Woodhouse, *Extended X-ray-absorption and electron–energy-loss fine-structure studies of the local atomic structure of amorphous unhydrogenated and hydrogenated silicon carbide*, Phys. Rev. B, 38 (1988), pp. 13099–13106.

[10] C. Meneghini, F. Boscherini, F. Evangelisti, and S. Mobilio, *Structure of a-$Si_{1-x}C_x$:H alloys by wide-angle X-ray scattering: Detailed determination of first- and second-shell environment for Si and C atoms*, Phys. Rev. B 50 (1994), pp. 11535–11545.

[11] P.C. Kelires, *Short-range order and energetics of disordered silicon–carbon alloys*, Phys. Rev. B 46 (1992), pp. 10048–10061; P.C. Kelires, *Structure and chemical ordering in amorphous silicon carbide alloys*, Europhys. Lett., 14 (1991), pp. 43–48; P.C. Kelires and P.J.H. Denteneer, *Theory of electronic properties of amorphous silicon–carbon alloys: Effects of short-range disorder*, Solid State Commun., 87 (1993), pp. 851–855; P.C. Kelires and P.J.H. Denteneer, *Total-energy and entropy considerations as a probe of chemical order in amorphous silicon carbide*, J. Non-Cryst. Solids, 231 (1998), pp. 200–204.

[12] J. Tersoff, *Chemical order in amorphous silicon carbide*, Phys. Rev. B 49 (1994), pp. 16349–16352.

[13] F. Finocchi, G. Galli, M. Parrinello, and M. Bertoni, *Microscopic structure of amorphous covalent alloys probed by* ab initio *molecular dynamics: SiC*, Phys. Rev. Lett. 68 (1992), pp. 3044–3047.

[14] V.I. Ivashenko, P.E.A. Turchi, V.I. Shevshenko, L.A. Ivashenko, and G.V. Rusakov, *Tight-binding molecular-dynamics simulations of amorphous silicon carbides*, Phys. Rev. B 66 (2002), 195201.

[15] J.P. Rino, I. Ebbsjö, P.S. Branicio, R.K. Kalia, A. Nakano, F. Shimojo, and P. Vashishta, *Short- and intermediate-range structural correlations in amorphous silicon carbide: A molecular dynamics study*, Phys. Rev. B 70 (2004), 045207.

[16] R. Devanathan, F. Gao, and W.J. Weber, *Atomistic modeling of amorphous silicon carbide using a bond-order potential*, Nucl. Instr. Meth. B 255 (2007), pp. 130–135.

[17] D.W. Brenner, *Empirical potential for hydrocarbons for use in simulating the chemical vapor deposition of diamond films*, Phys. Rev. B 42 (1990), pp. 9458–9464.

[18] B. Delley, *An all-electron numerical method for solving the local density functional for polyatomic molecules*, J. Chem. Phys. 92

(1990), pp. 508–517, B. Delley, *From molecules to solids with the DMol^3 approach*, J. Chem. Phys. 113 (2000), pp. 7756–7764. DMol^3 is implemented in the Materials Studio suite®.

[19] Z. Lin and J. Harris, *A localized-basis scheme for molecular dynamics*, J. Phys. Condens. Matter 4 (1992), pp. 1055–1080.

[20] X.P. Li, J. Andzelm, J. Harris, and A.M. Chaka, Chapter 26, in *American Chemical Society*, Ziegler, ed., Anaheim Symposium, 1996.

[21] S.H. Vosko, L. Wilk, and M. Nusair, *Accurate spin-dependent electron liquid correlation energies for local spin density calculations: A critical analysis*, Can. J. Phys. 58 (1980), pp. 1200–1211.

[22] The Goodfellow web site information about Nicalon® ($Si_{0.5}C_{0.5}$) physical properties: http://www.goodfellow.com/csp/active/STATIC/A/Silicon_Carbide_.HTML

[23] S.R. Elliot, *Physics of Amorphous Materials*, 2nd ed., Longman Scientific and Technical, 1990.

[24] A.J.C. Wilson, *International Tables for Crystallography C*, Kluwer Academic Publishers, 1995.